Polymer Degradation and Stability 112 (2015) 43–51

Contents lists available at ScienceDirect

Polymer Degradation and Stability

journal homepage: www.elsevier.com/locate/polydegstab

Comparison of intumescence mechanism and blowing-out effect in flame-retarded epoxy resins

Wenchao Zhang [a, b], Xiangdong He [a], Tinglu Song [a], Qingjie Jiao [b], Rongjie Yang [a, *]

[a] Beijing Institute of Technology, School of Materials, National Engineering Technology Research Center of Flame Retardant Materials, 5 South Zhongguancun Street, Haidian District, Beijing 100081, PR China
[b] Beijing Institute of Technology School of Mechatronical Engineering, PR China

ARTICLE INFO

Article history:
Received 13 August 2014
Received in revised form
7 November 2014
Accepted 30 November 2014
Available online 9 December 2014

Keywords:
Blowing-out effect
Intumescence
OPS/DOPO mixture
APP–MMT nanocomposite
Flame retardancy

ABSTRACT

Epoxy resins (EPs) have been flame-retarded by an APP–MMT nanocomposite (ammonium polyphosphate montmorillonite nanocomposite) and an OPS/DOPO (octaphenyl polyhedral oligomeric silsesquioxane/9,10-dihydro-9-oxa-10-phosphaphenanthrene-10-oxide) mixture, respectively. The flame retardancies and efficiencies of these systems have been investigated by LOI, UL-94, and cone tests. The OPS/DOPO mixture (blowing-out effect) was found to be more efficient for improving LOI, UL-94, p-HRR, and THR. However, 10 wt.% of the APP–MMT nanocomposite (intumescence mechanism) showed good flame retardancy and higher efficiency in reducing TSR. The flame retardancy mechanisms of the APP–MMT nanocomposite and the OPS/DOPO mixture have been investigated by TGA–FTIR, PY–GC/MS, FTIR, and SEM analyses. The results indicate that the APP–MMT nanocomposite accelerated the decomposition of epoxy resins, with most of the pyrolytic products consisting of small molecules. Furthermore, the melt viscosities of the pyrolytic residues correspond to the rate of gas release, which allows the formation of an intumescent and firm char layer. The OPS/DOPO mixture caused the epoxy resin to decompose rapidly, giving complex pyrolytic products. Moreover, EP/OPS/DOPO rapidly produced –Si–O–C– or –Si–O–P(=O)–C– cross-linked structures in the condensed phase under the action of heat, leading to formation of solid carbonaceous char. Because EP/OPS/DOPO decomposed rapidly, the hard char layer could not swell to accommodate the released gases, and consequently blowing-out could occur. The differences between intumescence and the blowing-out effect are caused by differences in the structures of the char layers and the rates of gas emission.

1. Introduction

Epoxy resins (EP) are very important thermosetting materials owing to their excellent mechanical and chemical properties [1–3]. They are widely applied in advanced composite matrices in the electronic/electrical industries, for which a highly flame-retardant grade is required. The fire risk remains a major drawback of these materials [4]. Halogen-containing compounds are effective flame retardants for epoxy resins. Their effect relies on the pyrolysis products of halogen-based flame retardants producing X• (Cl• or Br•) radicals and HX, which could scavenge the polymer degradation radicals (H• and •OH) in the gas phase, leading to an inhibition of flame propagation [5]. However, due to environmental concerns, some halogen-containing flame retardants have been gradually prohibited [6,7].

Phosphorus-containing compounds are important flame retardants for epoxy resins. They impart flame retardancy through flame inhibition in the gas phase and char enhancement in the condensed phase [8–10]. For example, ammonium polyphosphate (APP) is very effective for the flame retardation of epoxy resins [11]. Its principal flame-retardancy mechanism is that of “intumescence”, whereby flame retardants swell, bubble, and char on exposure to a flame and the carbonaceous porous foamed mass acts as a barrier to heat, air (O_2), and pyrolysis products. This is a typical condensed-phase flame-retardancy mechanism. However, the intumescent char layer cannot be created without the cooperation of appropriate gas release. Furthermore, the gas in the bubbles could retard heat transfer more effectively than a solid char layer [12–14].

Recently, our group reported a novel flame-quenching mechanism termed the “blowing-out effect”, which was found in epoxy resins flame retarded by DOPO-POSS, that depends on synergy between the gas phase and the condensed phase [15,16]. The

* Corresponding author. Tel.: +86 10 6891 2927.
E-mail address: yrj@bit.edu.cn (R. Yang).

http://dx.doi.org/10.1016/j.polymdegradstab.2014.11.017
0141-3910/

"blowing-out effect" has been described as follows: "after the sample was ignited, it showed an unstable flame for several seconds; with the pyrolytic gaseous products jetting outward from the condensed-phase surface, the flame was extinguished, it looked like the gas blew out the flame".

The intumescence mechanism and the blowing-out effect both depend on the synergy between the gas phase and condensed phase. In this research, epoxy resins (EPs) have been flame retarded by an APP–MMT nanocomposite and an OPS/DOPO mixture, allowing detailed comparison of the intumescence mechanism and the blowing-out effect. The respective combustion phenomena, extinction processes, gas-phase species, and condensed-phase structures have been investigated.

2. Experimental

2.1. Materials

Diglycidyl ether of biphenol A (DGEBA, E-44, epoxy equivalent = 0.44 mol/100 g) was purchased from FeiCheng DeYuan Chemicals CO., LTD. The 4, 4′-diaminodiphenylsulphone (DDS) was purchased from TianJin GuangFu Fine Chemical Research Institute. 9,10-dihydro-9-oxa-10-phosphaphenanthrene-10-oxide (DOPO) (Scheme 1) was purchased from Eutec Trading (Shanghai) Co. Ltd. Octaphenyl polyhedral oligomeric silsesquioxane (OPS) (Scheme 1) was synthesized in our laboratory with perfect T_8 cage [17]. Ammonium polyphosphate montmorillonite nanocomposite (APP–MMT nanocomposite) (Scheme 1) was prepared in our laboratory, which contain 6wt.% NaMMT [18].

2.2. Preparation of the cured epoxy resins

The cured epoxy resins were obtained using a thermal curing process. At first, the flame retardants were dispersed in DGEBA by mechanical stirring at 140 °C for 1 h and it would disperse in DGEBA. The mixture is homogeneous liquid always. After that, the curing agent DDS was then added relative to the amount of DGEBA. The equivalent weight ratio of DGEBA to DDS was 9:2. The epoxy resins were cured at 180 °C for 4 h. The LOI and UL-94 test samples were strips. The contents of the flame retardant in the EP composites are listed in Table 1.

2.3. Measurements

The limiting oxygen index (LOI) was obtained using the standard GB/T2406–93 procedure, which involves measuring the minimum oxygen concentration required to support candle-like combustion of plastics. An oxygen index instrument (Rheometric Scientific Ltd.) was used on samples of dimensions 100 × 6.5 × 3 mm^3. Vertical burning tests were performed using the UL-94 standard on samples of dimensions 125 × 12.5 × 3.2 mm^3. In this test, the burning grade of a material was classified as V-0, V-1, V-2 or unclassified, depending on its behavior (dripping and burning time).

Table 1
Composition of the investigated materials (wt.%).

Samples	Cured epoxy resins	APP–MMT	OPS	DOPO	P content	Si content
Pure EP	100.0	/	/	/	/	/
EP/APP–MMT	94.8	10.0	/	/	≈3.3	/
EP/OPS/DOPO	94.8	/	2.5	2.5	0.54	0.36

Cone calorimeter measurements were performed according to ISO 5660 protocol at an incident radiant flux of 50 kW/m^2. The equipment is Fire Testing Technology apparatus with a truncated cone-shaped radiator. The specimen (100 × 100 × 3 mm^3) was measured horizontally without any grids. Typical results from the cone calorimeter tests were reproducible within ±10%, and the reported parameters are the average of three measurements.

To investigate the flame retardancy efficiency of APP–MMT and OPS/DOPO, some calculations have been adopted. For the LOI, TTI, p-HRR, THR and TSR, the changes of their values (flame retarded EP composites minus pure EP) are divided by the content of flame retardants or flame retardant elements. Furthermore, the influence of matrix content changes has been considered for the calculated function of the p-HRR, THR and TSR.

Thermal gravimetric analysis (TGA) was performed with a Netzsch 209 F1 thermal analyzer, with the measurements carried out in a nitrogen atmosphere at a heating rate of 20 °C/min from 40 °C to 800 °C. 10 mg samples were used for each measurement, with a gas flow rate of 60 ml/min. The typical results from TGA were reproducible within ±1%, and the reported data are averages of three measurements. To detect the gas species given off, the TGA was coupled with a Fourier transform infrared spectrometer (TGA–FTIR, Nicolet 6700). The connection between the TGA and FTIR was effected with a quartz capillary held at a temperature of 200 °C.

Pyrolysis/gas-chromatograph/mass spectrometer (PY–GC/MS) analysis were performed using a vertical micro-furnace type double-shot pyrolyzer PY2020iD (Frontier Laboratories Ltd., Fukushima, Japan) attached to a GC/MS system (Agilent 6890). The evolved gases from pyrolysis were transferred on line to a gas chromatograph by using a capillary transfer line. The gas chromatograph was equipped with a low to-mid polarity-fused silica capillary column (J&W Scientific) of 30 m × 250 μm × 0.25 μm film thickness. The oven temperature was held at 80 °C for 3 min and then increased to 850 °C at 10 °C/min in the scan modus. The carrier gas was helium at a controlled flow of 1 ml/min. The detector consisted of an Agilent 5973 mass selective detector and electron impact mass spectra were acquired with 70 eV ionizing energy.

To investigate the condensed phase of the EP composites, all the cone calorimeter tests were stopped at 500 s. The residue was

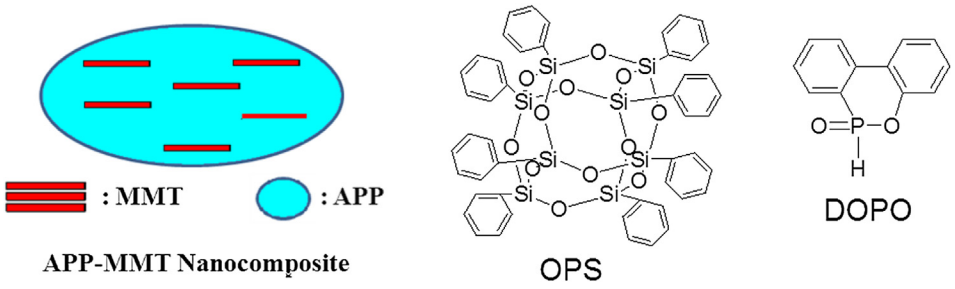

Scheme 1. Typical chemical structures of OPS, DOPO and APP–MMT nanocomposite.

Table 2
Flame retardancy of EP composites.

Samples	LOI (%)	UL-94 (3.2 mm)				Mechanism
		t_1 (s)	t_2 (s)	Dripping	Rating	
Pure EP	23.0	>120	/	Yes	NR	None
EP/APP–MMT	30.0	2	1	NO	V-0	Intumescence
EP/OPS/DOPO	31.0	4	2	NO	V-0	Blowing-out

cooled under room conditions. A sample of the exterior char of about 1 cm thickness was ground and analyzed by FTIR (Nicolet 6700) in ATR mode.

Scanning electron microscopy (SEM) experiments were performed with a Hitachi TM-3000 scanning electron microscope. The samples for SEM were sputtered on the surface without gold.

3. Results and discussion

3.1. Flame-retardant actions of APP–MMT nanocomposite and OPS/DOPO mixture

The effects of APP–MMT nanocomposite and OPS/DOPO mixture on the LOI values of DGEBA/DDS resins are presented in Table 2. When 10 wt.% APP–MMT was incorporated, corresponding to a flame-retardant element content of 3.3 wt.%, the LOI value increased from 23.0% to 30.0%. When 5 wt.% OPS/DOPO mixture was used instead, corresponding to a smaller flame-retardant element content of 0.9 wt.%, the LOI value of EP/OPS/DOPO increased from 23.0% to 31.0%.

The results of UL-94 tests are shown in Table 2. The flame retardancies of the EP resins were clearly improved with increased loadings of APP–MMT or OPS/DOPO mixture. For pure EP, dripping was observed, and self-extinguishing was not observed during the UL-94 test. From Table 2, it is clear that the EP resin with APP–MMT attained good flame retardancy, showing no dripping, quick self-extinguishing, and a UL-94 V-0 rating. When the OPS/DOPO mixture was used in the EP resin, the flame retardancy was also clearly enhanced, with very short flame-out times (t_1 and t_2) and very rapid self-extinguishing being observed.

As we expected, the intumescence phenomenon was observed in the EP/APP–MMT sample during the LOI and UL-94 tests, whereas the blowing-out effect was observed in the EP/OPS/DOPO sample during these tests. Fig. 1 shows photographs of sample bars of the EP composites after UL-94 tests. In the case of the pure EP bar,

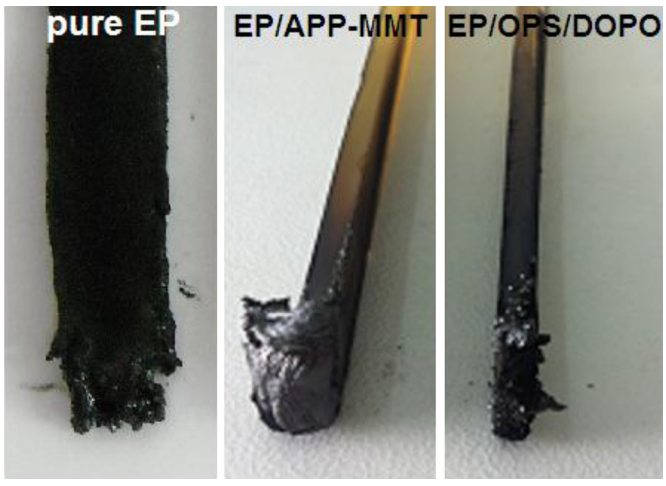

Fig. 1. Photo of bars after UL-94 test of pure EP, EP/APP–MMT and EP/OPS/DOPO.

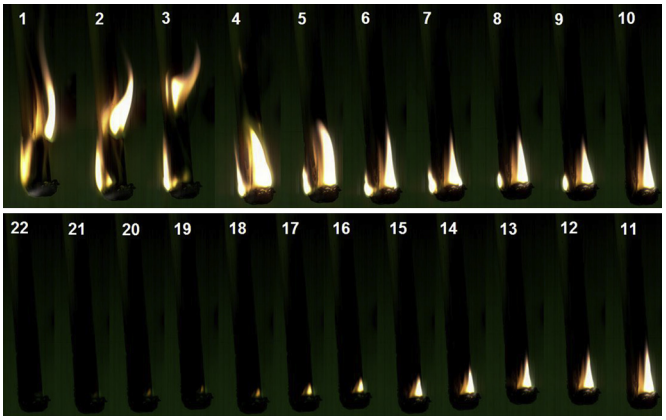

Fig. 2. Extinguishing process during the last seconds of high speed video for EP/APP–MMT.

little char was formed at its end, and its thermally decomposing surface was directly exposed. For EP/APP–MMT, intumescent char was clearly seen to cover the bottom of the sample rod. This char layer served to protect the unburned sample. For EP/OPS/DOPO, a rigid char-brick with the same dimensions as the original sample was observed. Similar char morphologies were obtained from DGEBA/DDS and DGEBA/*m*-PDA resins flame-retarded by DOPO-POSS in our previous research, which showed an obvious blowing-out effect [19,20].

The intumescence mechanism and the blowing-out effect not only yield residues with different morphologies, but their combustion and extinguishing processes are also completely different. Fig. 2 shows photographs of the last seconds of the combustion and extinguishing processes for EP/APP–MMT. It can be observed that an intumescent char layer was created during the combustion. Due to this layer, the flame was stable and remained on the surface of the char. However, with time, the flame gradually decreased and was eventually extinguished. The stable and decreased flame indicated that the intumescent char layer protected the unburned

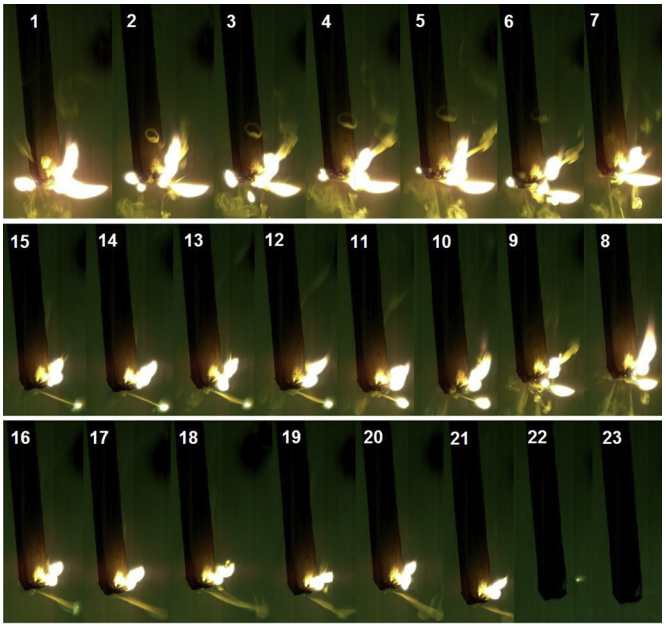

Fig. 3. Extinguishing process during the last seconds of high speed video for EP/OPS/DOPO.

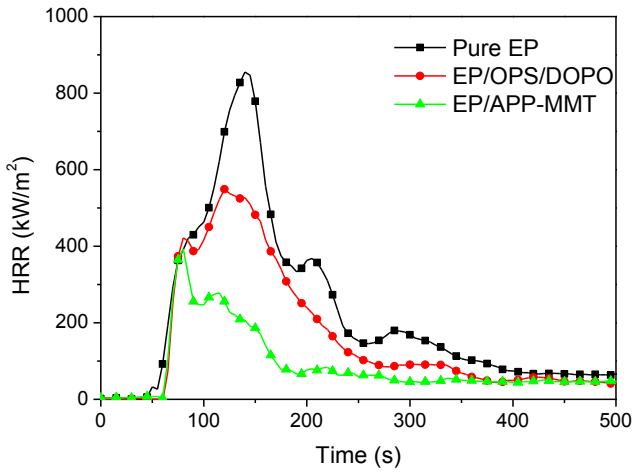

Fig. 4. Heat release rate curves of the flame retarded EP composites.

matrix well, reducing the supply of flammable products from the decomposition zone. Fig. 2 shows the extinction process of intumescence flame retardancy in detail.

Fig. 3 shows photographs of the last seconds of the combustion and extinguishing processes for EP/OPS/DOPO, from which a clear and powerful blowing-out effect is evident. The flame from EP/OPS/DOPO was mobile and several flames were observed on the char, which emerged from holes in the surface and sprayed in different directions. These "sting-outs" were caused by ignition of the jetting pyrolytic gases. As shown in Fig. 3, the pyrolytic gases jetted out very drastically from the char layer, such that the flame was pushed off the surface and left the unburnt residue. When the jetting of the gases was strong enough, the flame was extinguished immediately. This is the typical blowing-out effect.

The flame-retardant actions discussed above indicate that the intumescence mechanism and the blowing-out effect can impart DGEBA/DDS resin with similar LOI values and UL-94 ratings. However, as shown in Figs. 2 and 3, their flame-retardancy phenomena and mechanisms are quite different.

3.2. Cone calorimeter analysis

Cone calorimeter tests were conducted to investigate the effects of APP–MMT and OPS/DOPO on the fire behavior of DGEBA/DDS resin. The measured combustion parameters included time to ignition (TTI), heat release rate (HRR), peak of heat release rate (p-HRR), total heat release (THR), total smoke release (TSR), and average effective heat of combustion (AEHC).

TTI is used to determine the influence of a flame retardant on ignitability. Clear increases in TTI were observed after loading EP composites with APP–MMT or OPS/DOPO. Their TTI increased from 50 s to 60 s and 58 s, respectively. These increases in TTI are very valuable for enhancement of the flame-retardancy properties of epoxy resins.

Table 3
Cone calorimeter data for the EP composites.

Samples	TTI (s)	p-HRR (kW/m^2)	THR (MJ/m^2)	TSR (m^2/m^2)	Residues (%)	Mean EHC (MJ/kg)
Pure EP	50	860	112	4182	7	31
EP/APP–MMT	60	393	33	1522	39	18
EP/OPS/DOPO	58	540	82	3786	12	23

Table 4
The calculated function of each 1wt.% flame retardants.

Samples	LOI (%)	TTI (s)	p-HRR (kW/m^2)	THR (MJ/m^2)	TSR (m^2/m^2)	Mechanism
APP–MMT	+0.7	+1.0	−38.1	−6.78	−224.2	Intumescence
OPS/DOPO	+1.6	+1.6	−55.4	−4.88	−37.4	Blowing-out

HRR curves of the DGEBA/DDS resins are presented in Fig. 4. It can be seen that the pure EP burned rapidly after ignition and the HRR reached a sharp peak with a p-HRR of 860 kW/m^2. As shown in Fig. 4 and Table 3, when 10 wt.% APP–MMT was incorporated, the p-HRR of the DGEBA/DDS composite was clearly reduced from 860 kW/m^2 to 393 kW/m^2, that is, by more than 50%. For DGEBA/DDS with 5 wt.% OPS/DOPO, the p-HRR of the EP/OPS/DOPO was reduced by about 37% from 860 kW/m^2 to 540 kW/m^2. Another promising result was that the EP/APP–MMT showed the lowest THR, corresponding to about a 70% reduction due to the intumescent flame retardancy. Meanwhile, the THR of EP/OPS/DOPO was reduced by about 26% from 112 MJ/m^2 to 82 MJ/m^2 due to the blowing-out effect. The smoke release data in Table 3 show that APP–MMT significantly reduced the TSR of the EP resin from 4182 m^2/m^2 to 1522 m^2/m^2. For EP/OPS/DOPO, however, the TSR showed only a small reduction from 4182 m^2/m^2 to 3786 m^2/m^2. Thus, in this research, APP–MMT showed a better smoke suppression effect than OPS/DOPO. This may be attributed to APP–MMT increasing the char yield from the epoxy resin (TGA section), resulting in lower smoke release. It is acknowledged that phosphorus-containing flame retardants can exert a condensed-phase effect as well as a gas-phase effect [21–23]. From Table 3, it can be seen that the amounts of residue from EP/APP–MMT and EP/OPS/DOPO were increased, whereas the AEHC were reduced compared to those of pure EP. Thus, the flame-retardant effects of APP–MMT and OPS/DOPO are partly exerted in the gas phase. We also note that the AEHC of EP/APP–MMT was lower than that of EP/OPS/DOPO. We assume that this was because EP/APP–MMT contained 2.76% more phosphorus than EP/OPS/DOPO.

3.3. Flame-retardancy efficiencies of APP–MMT and OPS/DOPO

In cone analysis, APP–MMT (intumescence mechanism) showed better flame retardancy than OPS/DOPO (blowing-out effect) in EP resin, as manifested in lower p-HRR, THR, and TSR. However, it should be borne in mind that the content of APP–MMT was 10 wt.%, of which the phosphorus content was about 3.3 wt.%, whereas the content of OPS/DOPO was 5 wt.%, of which the phosphorus and silicon contents were only about 0.9 wt.%. Therefore, the relative efficiencies of these flame retardants and their flame-retardant element contents were investigated in detail. Tables 4 and 5 summarize the calculated functions of each 1 wt.% of flame retardant or flame-retardant elements.

As shown in Table 2, 10 wt.% APP–MMT increased the UL-94 rating of EP resin from no rating to V-0. For the OPS/DOPO mixture, just 5 wt.% addition was sufficient to obtain the same result. As shown in Table 4, 1 wt.% of APP–MMT enhanced the LOI value of EP resin by about 0.7%, whereas 1 wt.% of OPS/DOPO had a

Table 5
The calculated function of each 1wt.% flame retardant elements.

Samples	LOI (%)	TTI (s)	p-HRR (kW/m^2)	THR (MJ/m^2)	TSR (m^2/m^2)	Mechanism
APP–MMT (P)	+2.1	+3.0	−115.5	−20.5	−679.3	Intumescence
OPS/DOPO (P + Si)	+8.9	+8.9	−307.8	−27.1	−207.6	Blowing-out

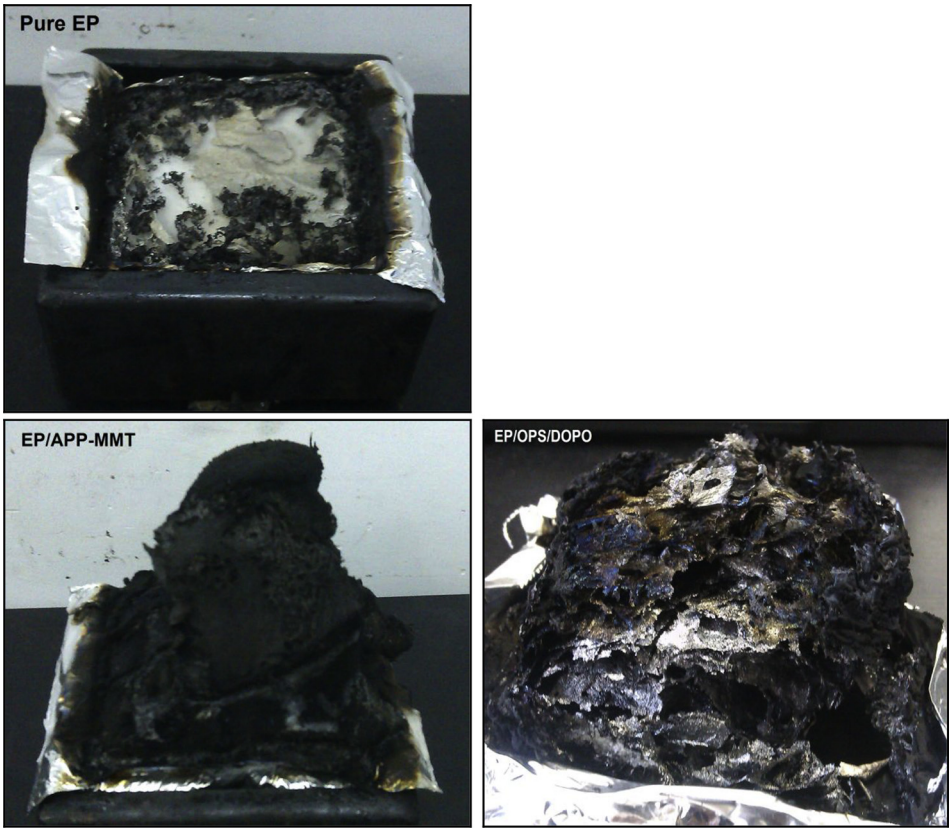

Fig. 5. Photographs of chars from EP composites after the cone calorimeter tests.

greater enhancing effect of about 1.6%. From the LOI and UL-94 results, we can conclude that the blowing-out effect due to OPS/DOPO has higher flame-retardant efficiency for epoxy resins than the intumescence mechanism due to APP–MMT. The cone analysis data in Table 4 also indicate that OPS/DOPO showed higher efficiency than APP–MMT in reducing the p-HRR. However, it is also apparent that APP–MMT showed better efficiency than OPS/DOPO in reducing the THR and TSR of EP resin. This result may be attributed to the fact that 5 wt.% OPS/DOPO contained only 0.9 wt.% phosphorus and silicon, which favors formation of a stable char layer, whereas the 10 wt.% APP–MMT contained 3.3 wt.% phosphorus. As shown in Table 5, if we consider only the efficiencies of the flame-retardant elements, OPS/DOPO showed better performance than APP–MMT in terms of THR data. In terms of TSR, APP–MMT showed better performance than OPS/DOPO. This may have been due to the EP/APP–MMT forming a compact intumescent char layer, as shown in Fig. 5, which could better protect the unburned matrix and prevent smoke emission. For EP/OPS/DOPO, however, the rapid release of pyrolysis products is advantageous for the blowing-out effect to break the plate-like char layer, but also causes more smoke emission.

This research on APP–MMT and OPS/DOPO is only a part of our investigations of the flame-retardancy efficiencies of the intumescence mechanism and the blowing-out effect, but from the obtained results, we can conclude that the blowing-out effect has a good flame-retarding effect on epoxy resins, which is due to a mechanism distinct from that of intumescence.

3.4. TGA of the cured epoxy resins

In order to reveal the differences between the intumescent mechanism and the blowing-out effect, the thermal stabilities of the EP composites were investigated by TGA. The relevant thermal decomposition data, including values of T_{onset}, defined as the temperature at which 5% weight loss occurs; T_{max}, defined as the temperature of maximum weight loss rate; and the char residue at 800 °C, are given in Table 6.

According to the TGA data, it is clear that both the APP–MMT nanocomposite and OPS/DOPO mixture lowered the onset temperature for epoxy resin decomposition. Furthermore, as shown by the DTG curves, the decomposition rate of EP/APP–MMT was the highest, the gas release rate being suitable to swell the char layer. The large intumescent char layer of EP/APP–MMT (Fig. 5) created during the cone test confirmed that APP–MMT promoted the swelling process thereof and helped to create a layer with high thermal stability. The fast gas release rate and the large amount of residue are key features for the intumescent flame retardancy. For EP/OPS/DOPO, T_{onset} and T_{max} were a little lower than those of pure EP, indicating that OPS/DOPO had a small effect on the thermal stability of the EP matrix. However, as shown in the DTG curves in Fig. 6, the decomposition rate of EP/OPS/DOPO was a little slower than that of pure EP. As shown in Fig. 1, the char layer of EP/OPS/DOPO retained its original shape, without showing intumescence. When this char layer cannot accommodate the abundant gas emission, the pyrolytic gases will break through it and jet out.

Table 6
TGA data of EP composites in nitrogen.

Samples	T_{onset} (°C)	T_{max} (°C)	Residues at 800 °C (%)
Pure EP	398	444	12.3
EP/APP–MMT	347	376	30.6
EP/OPS/DOPO	380	414	20.8

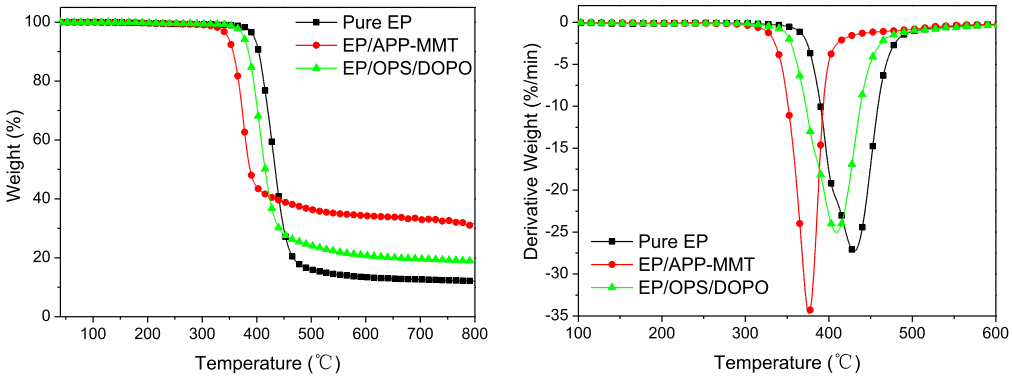

Fig. 6. TGA and DTG curves of EP composites in N_2.

Under these circumstances, the blowing-out effect will occur, especially in UL-94 and LOI tests. The rate of gas release and the structure of the char layer are important determining factors for the occurrence of intumescent flame retardancy or the blowing-out effect.

3.5. Analysis of the pyrolytic gaseous products

3.5.1. TGA–FTIR

In order to further investigate the differences between the intumescence mechanism and the blowing-out effect, the pyrolytic gas species from pure EP, EP/APP–MMT, and EP/OPS/DOPO were tested by TGA–FTIR. The FTIR spectra of the pyrolytic gaseous products at T_{max} are shown in Fig. 7. The assignments of the absorbance peaks are presented in Table 7.

The major pyrolytic gases detected from the decomposition of EP/APP–MMT and EP/OPS/DOPO composites were phenol derivatives/water (ν = 3650 cm^{-1}), aromatic components (ν = 3036, 1604, 1510, and 1340 cm^{-1}), aliphatic components (ν = 2972, 2930 and 2869 cm^{-1}), and ester/ether components (ν = 1748, 1257, and 1181 cm^{-1}) [24]. These results indicate that the gaseous species evolved from the flame-retarded epoxy resins were similar to those from pure EP. As shown in Fig. 7, although the gaseous species from the EP/APP–MMT composite were similar to those from the EP/OPS/DOPO composite, the former produced some NH_3 (ν = 967 and 932 cm^{-1}), originating from its ammonium cations [18]. In addition, no characteristic absorption bands due to phosphorus-containing moieties were detected in the spectra of the gaseous products from APP–MMT or OPS/DOPO in the epoxy resin composites. It is probable that some new absorption bands, for example at ν = 1260 (P═O) and 1118 cm^{-1} (–P–O–P–O–), coincide with the gaseous products evolved by EP degradation.

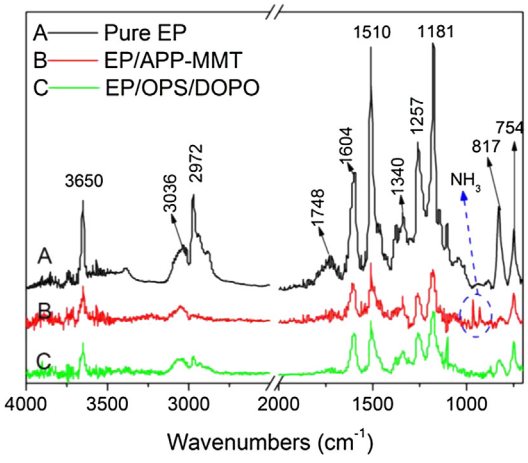

Fig. 7. FTIR spectra of pyrolytic products of EP composites at T_{max}.

Releases of aromatic and aliphatic components as a function of temperature for the epoxy resin composites are shown in Fig. 8, from which it is clear that those from EP/APP–MMT occurred earlier than those from EP/OPS/DOPO. This result corresponds well with the lower decomposition temperature of EP/APP–MMT compared to that of EP/OPS/DOPO, as shown by the TGA traces in Fig. 6. Furthermore, it is also apparent from Fig. 8 that the rates of release of aliphatic and aromatic components from EP/APP–MMT and EP/OPS/DOPO were different. Especially for the aliphatic components, the rates of release from EP/OPS/DOPO were obviously faster than those from EP/APP–MMT.

3.5.2. PY–GC/MS

Whereas TG–FTIR only provides information on the functional groups present in the pyrolysis products, mass spectrometry can reveal their precise composition. Thus, the exact compositions of the EP/APP–MMT and EP/OPS/DOPO degradation products were determined by PY–GC/MS. The volatilization profiles at maximum release intensity of pyrolytic products, represented as ion current, of the fragments originating from the thermal degradation of the EP composites are shown in Fig. 9. Possible structural assignments are listed in Table 8.

In Fig. 9, intense signals of species with different mass-to-charge ratios (m/z) at the maximum release intensity of pyrolytic products can be observed. The fragments at m/z 29 and 39 can be ascribed to aliphatic components. Those at m/z 51, 65, 66, and 77 can be ascribed to aromatic components. Phenol (m/z 94), methylphenol (m/z 107), ethylphenol (m/z 119, 121), and bisphenol A (m/z 228, 213) can also be identified. In Table 8, we can only give partial possible structures of the pyrolysis products as many isomers are

Table 7
Assignment of FTIR spectra of pyrolytic gases of epoxy resins.

Wavenumber (cm^{-1})	Assignment
3650	O–H stretching vibration of C_{Ar}–OH or water
3036	C_{Ar}–H stretching vibration of aromatic compound
2972	R–CH_2–R, R–CH_3 stretching vibration of aliphatic components
1748	C═O stretching vibration of compounds containing carbonyl
1604, 1510, 1340	aromatic rings vibration
1257, 1181, 1052	C–O stretching vibration
817, 754	C_{Ar}–H deformation vibration

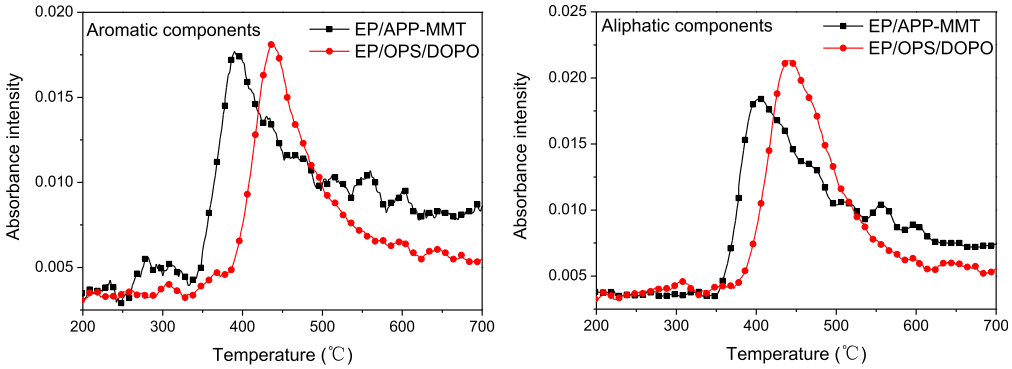

Fig. 8. The aromatic and aliphatic components release with temperature according to TG–FTIR spectra of EP composites.

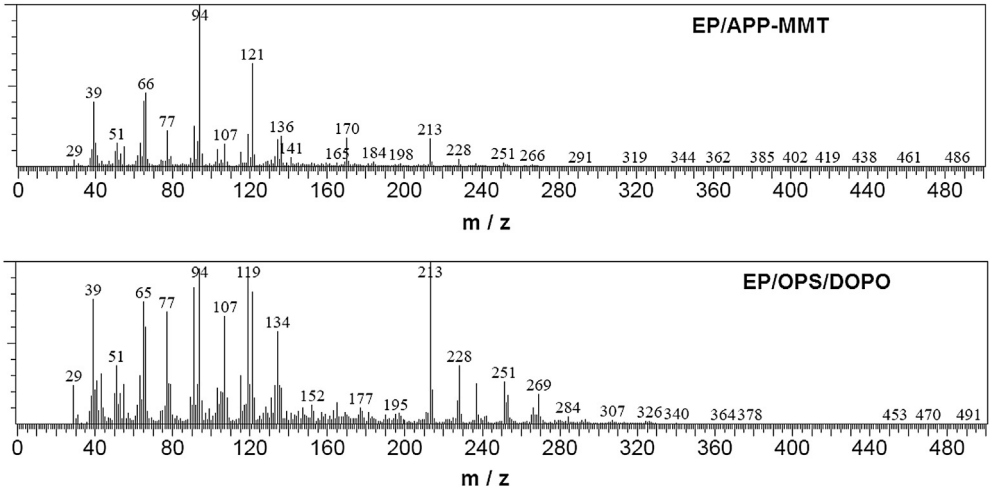

Fig. 9. The mass spectrum of EP/APP–MMT and EP/OPS/DOPO at maximum pyrolytic products release intensity.

likely to be present. However, these pyrolysis products from the EP composites correspond well to the TGA–FTIR results.

As shown in Fig. 9, the signals of the gaseous species from EP/APP–MMT and EP/OPS/DOPO at maximum release intensity of pyrolytic products were almost the same. However, the relative concentrations of these gas species were different. For EP/APP–MMT, the relative concentration of phenol (*m*/*z* 94) was the highest, and those of the fragments at *m*/*z* 39, 66, and 121 were also high. The relative concentrations of the other fragments were very low, and there were no obvious fragments at *m*/*z* > 200. This result indicates that the molecular chain of EP/APP–MMT decomposed completely into fragments of low molecular weight. For EP/OPS/DOPO, the relative concentrations of phenol (*m*/*z* 94), ethylphenol (*m*/*z* 119), and bisphenol A (*m*/*z* 213) were the highest and almost the same. The relative concentrations of the fragments at *m*/*z* 39, 65, 77, 107 and 134 were also high. Furthermore, larger fragments at *m*/*z* 228, 251, and 269 could also be detected. These results indicate that the pyrolytic products from EP/OPS/DOPO were complex and contained some larger chain segments, in marked contrast to the fragmentation of EP/APP–MMT.

Table 8
Possible structural assignments in the PY–GC–MS of EP/APP–MMT and EP/OPS/DOPO.

m/*z*	Structures	*m*/*z*	Structures
29	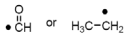	94	
39		107	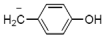
51		119	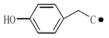
65		121	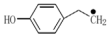
66		213	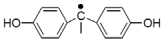
77		228	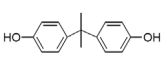

high. The relative concentrations of the other fragments were very low, and there were no obvious fragments at *m*/*z* > 200. This result indicates that the molecular chain of EP/APP–MMT decomposed completely into fragments of low molecular weight. For EP/OPS/DOPO, the relative concentrations of phenol (*m*/*z* 94), ethylphenol (*m*/*z* 119), and bisphenol A (*m*/*z* 213) were the highest and almost the same. The relative concentrations of the fragments at *m*/*z* 39, 65, 77, 107 and 134 were also high. Furthermore, larger fragments at *m*/*z* 228, 251, and 269 could also be detected. These results indicate that the pyrolytic products from EP/OPS/DOPO were complex and contained some larger chain segments, in marked contrast to the fragmentation of EP/APP–MMT.

Considering the different components of the pyrolytic products from EP/APP–MMT and EP/OPS/DOPO, and their different decomposition processes observed by TGA, we conclude that APP–MMT nanocomposite causes EP to decompose more rapidly, with the majority of the pyrolytic products being small molecules; larger chain segments remain in the condensed phase and form the char layer. This kind of char layer will swell under the action of appropriate pyrolytic gases. In this research, EP/APP–MMT was found to create a perfect intumescent char layer to retard the flame. For the EP/OPS/DOPO, OPS/DOPO mixture make EP decompose similar to that of pure EP. This decomposition leads complex pyrolytic products, which contains micromolecule and big chain segment that have been proved by the PY–GC/MS analysis. When the char layer cannot contain the gaseous products, the pyrolytic gases will jet out to produce the blowing-out effect. It is that the high instantaneous

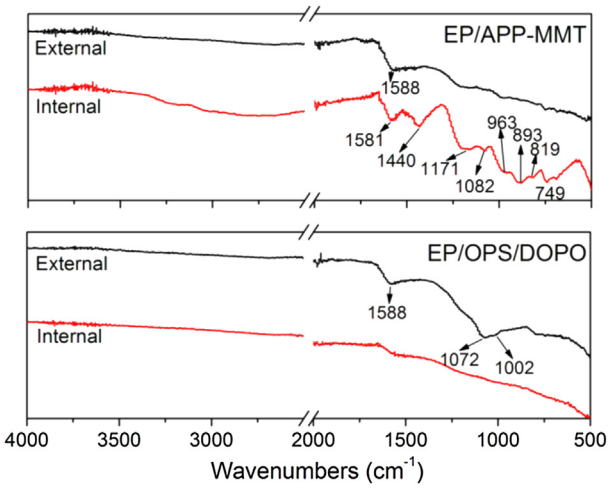

Fig. 10. FTIR spectra of the residues of EP composites after cone testing.

concentration of gaseous products leads the gaseous mixture above flammability limits resulting in flame extinction.

3.6. Analysis of pyrolytic residues

FTIR spectra of the char residues are shown in Fig. 10. The only absorbance of the external char of EP/APP–MMT is a broad band at ν = 1588 cm^{-1}, indicating the formation of polyaromatic carbon species [24]. No obvious P–O or P═O absorbances can be discerned in the FTIR spectrum. The FTIR spectrum of the internal char from EP/APP–MMT features peaks at ν = 1581, 1440, 1171, 1082, 963, 893, 819, and 749 cm^{-1}, which are characteristic absorption peaks of pyrolytic residues of EP networks and APP, as reported in our previous papers [24,25]. Such residues with extensive EP networks show lower viscosity than chars composed of polyaromatic carbon species. SEM images of the char from EP/APP–MMT are shown in Fig. 11. It can be seen that the interior char is honeycomb-like, with numerous closed bubbles separated by very thin walls. The exterior of the char shows a cracked layer that may have been broken by heat and gas release. The internal honeycomb char layer could be attributed to the low melt viscosity of the condensed phase, which is suitable for swelling induced by gas release during combustion.

For EP/OPS/DOPO, the external char again shows a broad band at ν = 1588 cm^{-1}, indicating the formation of polyaromatic carbon species. Furthermore, two absorption peaks at ν = 1002 and 1072 cm^{-1} can be ascribed to Si–O–Si–O and –P(═O)–O–Si– structures, respectively [19,20,26–29].

The internal residue from EP/OPS/DOPO shows no obvious absorption peak in its FTIR spectrum, which implies that it mostly consists of inorganic carbon. Such residues tend to show high viscosity, making them difficult to swell. As shown in Fig. 11, the exterior char from EP/OPS/DOPO shows a continuous perforated layer, whereas its interior char shows a continuous and rugged phase, with microstructures containing fine pores. These morphologies of the char layers may be attributed to the increased viscosity of the condensed phase, and seemingly favor the blowing-out effect.

3.7. Mechanistic interpretation

The main differences between the intumescence mechanism and the blowing-out effect in retarding flames from EP may be summarized on the basis of the above experimental results. In the

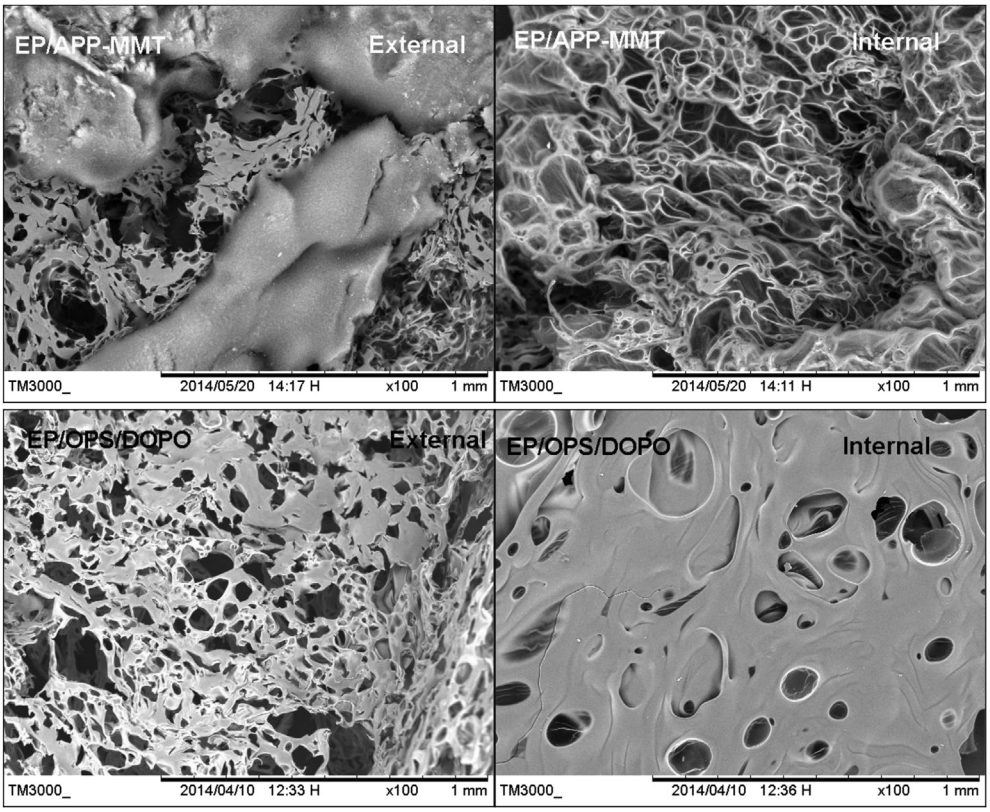

Fig. 11. Residue morphologies of EP composites.

case of the intumescence mechanism, the EP/APP–MMT composite decomposes early and rapidly. The viscosity of the pyrolytic residue matches the rate of gas release, which favors the formation of an intumescent and firm char layer. In the case of the blowing-out effect, EP/OPS/DOPO rapidly produces –Si–O–C– or –Si–O–P(=O)–C– cross-linked structures in the condensed phase under the action of heat, leading to formation of solid carbonaceous char. As EP/OPS/DOPO decomposes quickly, this hard char layer cannot accommodate the gases and blowing-out will suddenly occur. Hence, the differences between the intumescence mechanism and the blowing-out effect are caused by the different structures of the char layers and the rates of gas emission.

4. Conclusions

The intumescence mechanism and blowing-out effect are observed when APP–MMT nanocomposite and OPS/DOPO mixture, respectively, are used to flame retard epoxy resins. In this research, both phenomena could make the LOI values of epoxy resins greater than 30% and impart a V-0 rating in UL-94 tests. Furthermore, their p-HRRs in cone tests were reduced by more than 37%. Due to the different mechanisms, the APP–MMT nanocomposite and OPS/DOPO mixture showed different efficiencies in improving the studied burning parameters. Thus, the OPS/DOPO mixture (blowing-out effect) showed higher efficiency for improving LOI, UL-94, p-HRR, and THR. However, the APP–MMT nanocomposite (intumescence mechanism) showed higher efficiency for improving TSR.

TGA–FTIR and PY–GC/MS analysis have shown that the OPS/DOPO mixture caused the epoxy resin to decompose fast, giving complex pyrolysis products. Conversely, APP–MMT caused the epoxy resin to decompose more rapidly, with the majority of the pyrolytic products being small molecules. Analysis of the condensed phase by SEM and FTIR confirmed that the intumescence mechanism caused the EP/APP–MMT composite to decompose earlier and rapidly. The melt viscosity of the pyrolytic residue matched the rate of gas release, which favored the formation of an intumescent and firm char layer. In the case of the blowing-out effect, EP/OPS/DOPO rapidly produced –Si–O–C– or –Si–O–P(=O)–C– cross-linked structures in the condensed phase under the action of heat, leading to formation of a solid carbonaceous char. Because EP/OPS/DOPO decomposed fast, this hard char layer could not contain the released gases and blowing-out suddenly occurred. Hence, the differences between the intumescence mechanism and the blowing-out effect are caused by the different structures of the char layers and the rates of gas emission.

Acknowledgment

This project was funded byNational Natural Science Foundation of China (No. 51273023) and China Postdoctoral Science Foundation (No. 2014M550023).

References

[1] Wang X, Hu Y, Song L, Xing WY, Lu HD, Lv P, et al. Flame retardancy and thermal degradation mechanism of epoxy resin composites based on a DOPO substituted organophosphorus oligomer. Polymer 2010;51:2435–45.
[2] Liu HZ, Zheng SX, Nie KM. Morphology and thermomechanical properties of organic-inorganic hybrid composites involving epoxy resin and an incompletely condensed polyhedral oligomeric silsesquioxane. Macromolecules 2005;38:5088–97.
[3] Brus J, Urbanová M, Strachota A. Epoxy networks reinforced with polyhedral oligomeric silsesquioxane: structure and segmental dynamics as studied by solid-state NMR. Macromolecules 2008;41:372–86.
[4] Liu R, Wang XD. Synthesis, characterization, thermal properties and flame retardancy of a novel nonflammable phosphazene-based epoxy resin. Polym Degrad Stab 2009;94:617–24.
[5] Kiliaris P, Papaspyrides CD. Polymer/layered silicate (clay) nanocomposites: an overview of flame retardancy. Prog Polym Sci 2010;35:902–58.
[6] Chow WS, Neoh SS. Dynamic mechanical, thermal, and morphological properties of silane-treated montmorillonite reinforced polycarbonate nanocomposites. J Appl Polym Sci 2009;114:3967–75.
[7] Becker L, Lenoir D, Matuschek G, Kettrup A. Thermal degradation of halogen-free flame retardant epoxides and polycarbonate in air. J Anal Appl Pyrolysis 2001;60:55–67.
[8] Lejeune N, Dez I, Jaffres PA, Lohier JF, Madec PJ, Sopkova-de Oliveira Santos J. Synthesis, crystal structure and thermal properties of phosphorylated cyclotriphosphazenes. Eur J Inorg Chem 2008;1:138–43.
[9] Orme CJ, Klaehn JR, Harrup MK, Lash RP, Stewart FF. Characterization of 2-(2-methoxyethoxy)ethanol-substituted phosphazene polymers using pervaporation, solubility parameters, and sorption studies. J Appl Polym Sci 2005;97:939–45.
[10] Zhu L, Zhu Y, Pan Y, Huang YW, Huang XB, Tang XZ. Fully crosslinked poly[cyclotriphosphazene-co-(4,4′-sulfonyldiphenol)] microspheres via precipitation polymerization and their superior thermal properties. Macromol React Eng 2007;1:45–52.
[11] Camino G, Martinasso G, Costa L. Thermal degradation of pentaerythritol diphosphate, model compound for fire retardant intumescent systems. Part I. Overall thermal degradation. Polym Degrad Stab 1990;27:285–96.
[12] Lewin M. Physical and chemical mechanisms of flame retarding of polymers. In: Le Bras M, Camino G, Bourbigot S, Delobel R, editors. Fire retardancy of polymers – the use of intumescence. Cambridge: The Royal Society of Chemistry; 1998. p. 1–32.
[13] Le Bras M, Bourbigot S, Revel B. Comprehensive study of the degradation of an intumescent EVA-based material during combustion. J Mater Sci 1999;34:5777–82.
[14] Camino G, Costa L, Luda MP. Mechanistic aspects of intumescent fire retardant systems. Makromol Chem Makromol Symp 1993;74:71–83.
[15] Zhang WC, Li XM, Yang RJ. Novel flame retardancy effects of DOPO-POSS on epoxy resins. Polym Degrad Stab 2011;96:2167–73.
[16] Zhang WC, Li XM, Li LM, Yang RJ. Study of the synergistic effect of silicon and phosphorus on the blowing-out effect of epoxy resin composites. Polym Degrad Stab 2012;97:1041–8.
[17] Li LM, Li XM, Yang RJ. Mechanical, thermal properties, and flame retardancy of PC/ultrafine octaphenyl-POSS composites. J Appl Polym Sci. http://dx.doi.org/10.1002/app.35443.
[18] Yi DQ, Yang RJ. Ammonium polyphosphate/montmorillonite nanocompounds in polypropylene. J Appl Polym Sci 2010;118:834–40.
[19] Zhang WC, Li XM, Yang RJ. Blowing-out effect of epoxy composites flame-retarded by DOPO-POSS and its correlation with amide curing agents. Polym Degrad Stab 2012;97:1314–24.
[20] Zhang WC, Li XM, Fan HB, Yang RJ. Study on mechanism of phosphorus–silicon synergistic flame retardancy on epoxy resins. Polym Degrad Stab 2012;97:2241–8.
[21] Pawlowski KH, Schartel B. Flame retardancy mechanisms of triphenyl phosphate, resorcinol bis(diphenyl phosphate) and bisphenol bis(diphenyl phosphate) in polycarbonate/acrylonitrile-butadiene-styrene blends. Polym Int 2007;56:1404–14.
[22] Perret B, Pawlowski KH, Schartel B. Fire retardancy mechanisms of arylphosphates in polycarbonate (PC) and PC/acrylonitrile-butadiene-styrene. J Therm Anal Calorim 2009;97:949–58.
[23] Pawlowski KH, Schartel B, Fichera MA, Jager C. Flame retardancy mechanisms of bisphenol A bis(diphenyl phosphate) in combination with zinc borate in bisphenol A polycarbonate/acrylonitrile-butadiene-styrene blends. Thermochim Acta 2010;498:92–9.
[24] Yu D, Kleemeier M, Wu GM, Schartel B, Liu WQ, Hartwig A. Phosphorus and silicon containing low-melting organic-inorganic glasses improve flame retardancy of epoxy/clay composites. Macromol Mater Eng 2011;296:952–64.
[25] Wawrzyn E, Schartel B, Seefeldt H, Karrasch A, Jäger C. What reacts with what in bisphenol a polycarbonate/silicon rubber/bisphenol a bis(diphenyl phosphate) during pyrolysis and fire behavior? Ind Engin Chem Res 2012;51:1244–55.
[26] Zhang WC, Li XM, Yang RJ. Pyrolysis and fire behavior of epoxy resin composites based on a phosphorus-containing polyhedral oligomeric silsesquioxane (DOPO-POSS). Polym Degrad Stab 2011;96:1821–32.
[27] Liu Y-L, Chou C-I. The effect of silicon sources on the mechanism of phosphorusesilicon synergism of flame retardation of epoxy resins. Polym Degrad Stab 2005;90:515–22.
[28] Liu Y-L, Chie Y-C, Wu C-S. Preparation of silicon-/phosphorous-containing epoxy resins from the fusion process to bring a synergistic effect on improving the resins' thermal stability and flame retardancy. J Appl Polym Sci 2003;87:404–11.
[29] Hsiue G-H, Liu Y-L, Tsiao J. Phosphorus-containing epoxy resins for flame retardancy V: synergistic effect of phosphorus–silicon on flame retardancy. J Appl Polym Sci 2000;78:1–7.